# A MULTI-SCALE EPIDEMIC MODEL OF SALMONELLA INFECTION WITH HETEROGENEOUS SHEDDING

Simon Labarthe, Béatrice Laroche, Thao Nguyen, Bastien Polizzi, Florian Patout, Magali Ribot, T Stegmaier

**ESAIM: PROCEEDINGS AND SURVEYS, Vol. ?, 2019, 1-10**
Editors: Will be set by the publisher

# A MULTI-SCALE EPIDEMIC MODEL OF *SALMONELLA* INFECTION WITH HETEROGENEOUS SHEDDING *

S. Labarthe[1], B. Laroche[3], T. Nguyen[2], B. Polizzi[3], F. Patout[4], M. Ribot[5] and T. Stegmaier[7]

**Abstract.** ????

**Résumé.** ????

## Introduction

Salmonella infection is the most common vector of collective food poisoning in the developed world. As such, deciphering the mechanisms of infection in humans and animals is a fundamental step towards the design of efficient epidemiological policies, in order to reduce the burden on agrifood industry and healthcare systems resulting from Salmonella zoonoses. Salmonella is a bacterial genus composed of various pathogenic strains, that colonize and infect the digestive tract of farm livestock, such as chickens or pigs, representing a threat for human health ranging from food poisoning to typhoid fever. In this type of animal epidemic, it has been shown that the ability to excrete the pathogen in the environment (e.g. in water, food, or feces) and thus to contaminate other individuals in the farm varies from one individual to another. Some of them, called super-shedders, are permanent carriers and highly excreting the pathogen without being affected, thus causing most of the epidemic spread. This super-shedder phenotype, still poorly defined, is most probably the result of interactions between the host's immune response, the pathogen and the commensal intestinal flora. Recent studies [1] have identified key interactions between *Salmonella Typhimurium* and its host during infection. In the host's gut, pathogenic virulence factors promote the inflammation of the epithelium. The inflammatory process modifies the nutritional environment of the gut lumen which disturbs the ecological equilibrium of the microbiota and creates new niches that are targeted by the pathogen. The induced inflammation provides to the pathogen a competitive advantage, which can be sufficient to promote its proliferation and its transmission to another host. The aim of this paper is to propose a generic multiscale modeling framework of heterogeneous pathogen transmission in a livestock, accounting for the interaction dynamic between the commensal microbiota, the pathogen and the inflammatory

* *S. Labarthe and B. Laroche were supported by the One-Health EJP JRP-10 European grant. S. Labarthe also got support of the AgreenSkills+ fellowship programme which has received funding from the EU's Seventh Framework Programme under grant agreement Number FP7-609398 (AgreenSkills+ contract).*

[1] MaIAGE, INRA, Université Paris-Saclay, 78350 Jouy-en-Josas, France

[2] Laboratoire de Mathématiques de Besançon, UMR CNRS 6623, Université Bourgogne Franche-Comté

[3] Université Claude Bernard Lyon 1, CNRS UMR 5208, Institut Camille Jordan

[4] UMPA, Ecole Normale Supérieure de Lyon, UMR CNRS 5669

[5] Université d'Orléans, CNRS, UMR 7349 MAPMO

[6] Tabea Stegmaier

[7] Interdisziplinaren Forschungsgruppe zur Analyse biologischer Risiken, Universitat Hamburg

response at the intra-host level and transmission at between-host scale in a single animal population. This model is further extended at the metapopulation level, to model transmission between several populations.

The outline of the paper is the following. The single population model is described in section 1. The different scales and their interconnection are detailed. We start from an ODE equation modeling the intra-host evolution of the pathogen load with respect to time,including the host response. We next introduce a stochastic perturbation to this dynamics to account for biological variability. This SDE is used to derive a drift-diffusion PDE describing the evolution of a population density with respect to time and to pathogen load. The well-posedness of the model and asymptotic convergence towards a steady state is analyzed and an extension to the case with transmission of salmonella within the population through a reservoir is also proposed, leading to the coupling between a drift-diffusion PDE for the population and an ODE for the reservoir variable. Section 2 is devoted to some simulations of the two previous models, with or without a reservoir, and we observe that in both cases, the solution always converges towards a steady state. In section 3, some simulations of epidemic control strategies based on cleaning or drug treatment, are performed and compared. Cleaning is modeled through the addition of a term in the ODE for the reservoir variable, whereas drug treatment is described by the addition of a drift term in the population PDE equation. Then, in section 4, a compartment model taking into account some exchanges between populations is introduced and studied numerically. The model becomes in this section a large system that couples through transfer flux terms the models of the compartment dynamics composed of the previous drift-diffusion PDEs for the populations coupled to the ODE for the reservoir variables. Finally, some conclusive remarks and perspectives are given.

## 1. Mathematical models for a population structured by pathogen load

In this section, we will first present an ODE model which describes the evolution of pathogens in the gut for an individual. From this model, we will deduce a PDE for a population of individuals with pathogen loads, i.e. a drift-diffusion equation structured in pathogen load. We are able to prove the existence and uniqueness of solutions to this PDE and to compute explicitly the unique stationary state, which is reached asymptotically. This system is finally generalized by adding an ODE which takes into account the pathogens in the environment seen as a reservoir.

### 1.1. **A simple model of the pathobiome dynamics**

A simple way to model the pathobiome dynamics in the host gut is to consider two populations: the pathogen and its ecological competitors among the commensal gut bacteria. In order to build the equations, the following mechanisms are considered: the pathogens provoke an inflammatory response of the host, which affects the pathogens as well as the commensal bacteria. However, the inflammation causes an increase in the oxygen level near the gut epithelium, thus providing a competitive advantage to the pathogens. Indeed, the commensal microorganisms are mainly anaerobic, which means that they are highly sensitive to oxygen.

Let $p$ and $b$ be the concentrations of pathogens and competitors in the host gut. The ecological competition is modeled by the fact that these species share the same niche in the system, that is by the equation $p + b = \mathrm{K}$, where K is a positive constant modeling the carrying capacity of the host's gut for the corresponding niche, in the absence of any other limiting factor. This equation will lead to the absence of the unknown $b$ in the equations describing the evolution of the system.

Let $d$ be, as mentioned above, a deleterious signal targeted towards $b$, such as oxygen, resulting from the inflammatory response to the pathogens. The evolution of $b$ is modeled by the following equation :

$$b' = b(\mathrm{K} - b)\left(\mu - \alpha b - C_1 d\right),$$

where $\mu$, $\alpha$ and $C_1$ are positive. Here the growth rate of $b$ is proportional to the term $\mu(\mathrm{K} - b) = \mu p$, which induces a logistic term accounting for the competitive interaction between the commensal competitors and the pathogens. This growth rate is modulated by a factor $\left(1 - \frac{\alpha}{\mu} b - \frac{C_1}{\mu} d\right)$, where the term $1 - \frac{\alpha}{\mu} b$ represents a

growth limitation related to the actual environment in the gut, such as the presence of other competitors of $b$ or the basal immune system response. Asymptotically, this term may modify the theoretical trade-off between $b$ and $p$ to allow a coexistence of the pathogens and their competitors. The term $-\frac{C_1}{\mu}d$ accounts for the influence of the deleterious signal $d$ on the growth dynamics and on the equilibria.

Now, let us write the following equation, modeling the evolution of the signal $d$ with respect to time :

$$d' = \frac{1}{\tau}\left(-d + C_2\frac{p^n}{p^n + {p_\star}^n}\right).$$

In this equation, the presence of the pathogens directly promotes the host inflammatory response and induces the production of the deleterious signal $d$. This promotion is limited when the number of pathogens become very high; this is expressed through the sigmoidal function $C_2\frac{p^n}{p^n + {p_\star}^n}$ "centered" around the threshold $p_\star \in [0, \mathrm{K}]$, with $n \in \mathbb{N}^*$ an exponent controlling the stiffness of the sigmoid. In this equation, the parameter $\tau$ shows a time delay between the evolution of the pathogens and the evolution of the concentration of oxygen.

Consequently, applying the change of variable $p = \mathrm{K} - b$ and setting $A = \alpha\mathrm{K} - \mu$, the model equations read :

$$\begin{aligned} p' &= p(\mathrm{K} - p)\left(A - \alpha p + C_1 d\right), \\ d' &= \frac{1}{\tau}\left(-d + C_2\frac{p^n}{p^n + {p_\star}^n}\right). \end{aligned}$$

Finally, we assume that the dynamics of $d$ is very fast, that is $0 < \tau \ll 1$. Therefore, it is natural to assume that $d$ is at quasi-steady state, and to simplify the model into a single equation

$$p' = p(\mathrm{K} - p)\left(A - \alpha p + C\frac{p^n}{p^n + {p_\star}^n}\right), \tag{1}$$

where $C = C_1C_2$. We then get a monodimensional ODE on the pathogen only, that keeps track of the main drivers of Salmonella infection through its coefficients: 1) the parameter $A$ sums up microbial ecology characteristics by balancing the commensal growth rate $\alpha$ with the environmental harshness $\alpha K$, which is also taken into account by the parameter $\alpha$; 2) the parameter $C$ reflects the virulence of the host inflammatory response (the parameter $C_2$ describing the amount of deleterious signal produced during inflammation and $C_1$ its impact on commensals); 3) the host sensitivity to pathogens is shaped by the coefficients $p_\star$, that determines the amount of pathogen tolerated by the host, and the exponent $n$ that represents the virulence of the inflammation (a higher $n$ induces a sharper inflammative response to the pathogen presence, beneficiary to the pathogen).

Depending on the values of $A$, $\alpha$, $C$, $n$ and $p_\star$, this ordinary differential equation can possess from two to five steady states in the interval $[0, \mathrm{K}]$, including 0 and K, alternatively stable or unstable. Discarding the trivial situation in which only two steady states (K is stable, 0 is unstable) exist, the stability of the equilibria in the case of 3, 4 or 5 steady states in $[0, \mathrm{K}]$ is summarized in Table 1, when $A, \alpha$ and $C$ are positive. In that case and when there are two stable ($p_1$ and $p_3$) and three unstable (0, $p_2$ and K) steady states, the two stable steady states can be interpreted biologically as the concentrations of pathogens in low and high-shedders respectively.

### 1.2. **A model derived from individual stochastic variability**

From the previous ODE model, we obtain now an evolution equation for a whole population of individuals structured by pathogen loads.

Biological systems often exhibit intrinsic stochastic fluctuations in their dynamics. It therefore seems sensible to reformulate the model (1) as a stochastic differential equation (SDE)

$$d\,P = F(P)dt + \sigma dB, \tag{2}$$

| Value | Stability | | |
|---|---|---|---|
| | 3 steady states | 4 steady states | 5 steady states |
| 0 | unstable | unstable | unstable |
| $p_1$ | stable | stable | stable |
| $p_2$ | | unstable | unstable |
| $p_3$ | | | stable |
| K | unstable | stable | unstable |

TABLE 1. Stability of the steady states $0 < p_1 < p_2 < p_3 < \mathrm{K}$ when $A, \alpha$ and $C$ are positive.

where $P(t)$ is now a stochastic variable modeling the amount of pathogens in the gut, $dB$ is a gaussian unitary white noise, $\sigma > 0$ is the instantaneous standard deviation of the stochastic fluctuations in the model and the function $F$ is defined on $\mathbb{R}$ by

$$F(p) = \begin{cases} p(\mathrm{K}-p)\left(A - \alpha p + C\dfrac{p^n}{p^n + {p_\star}^n}\right), & \text{if } p \in [0,\mathrm{K}], \\ 0, & \text{otherwise.} \end{cases} \tag{3}$$

It can be easily checked that $F$ is uniformly Lipschitz on $\mathbb{R}$, and has linear growth. As $\sigma$ is constant, we can use standard results from SDE theory (see e.g. [2]) to obtain the so-called forward Kolmogorov equation of (2)

$$\begin{aligned} &\partial_t u(t,p) = -\partial_p(F(p)u(t,p)) + \frac{\sigma^2}{2}\partial^2_{pp}u(t,p), \\ &u(0,\ \cdot\ ) = u_{\mathrm{ini}}(\ \cdot\ ); \end{aligned}$$

the solution $u(t,p)$, defined on $L^2(\mathbb{R}^+ \times \mathbb{R})$, is the probability density function of $p(t)$ at time $t$, conditionally on the probability density of the initial pathogen population density function $u_{\mathrm{ini}}$.

However, this model is not quite satisfactory as brownian stochastic fluctuations make it possible to achieve realizations of $p(t)$ that are negative or greater than K. To avoid this, the SDE (2) has to be transformed into a SDE with reflecting boundary conditions which requires more sophisticated tools from stochastic process theory (see e.g. [3] for a quick introduction). The resulting forward Kolmogorov equation is modified in such a way that the solution space is now $L^2\left(\mathbb{R}^+, L^2\left(0,\mathrm{K}\right)\right)$ and its formulation is

$$\begin{aligned} &\partial_t u(t,p) = -\partial_p(F(p)u(t,p)) + \frac{\sigma^2}{2}\partial^2_{pp}u(t,p), \\ &\partial_p u(\cdot,0) = \partial_p u(\cdot,\mathrm{K}) = 0, \\ &u(0,\cdot) = u_{\mathrm{ini}}(\cdot) \in L^2(0,K), \quad \int_0^{\mathrm{K}} u_{\mathrm{ini}}(p)dp = 1. \end{aligned}$$

We now consider a very large population such that it can be described by a population density $s(t,p)$, meaning that $\int_a^b s(t,p)dp$ is the number of individuals with a pathogen load between $a$ and $b$ at time $t$. Define $s(t,p) = Nu(t,p)$ so that the total size of the population $N = \displaystyle\int_0^{\mathrm{K}} s(t,p)dp$ is constant. Then the population density $s$ satisfies the

following equations :

$$\partial_t s(t,p) = -\partial_p(F(p)s(t,p)) + \frac{\sigma^2}{2}\partial^2_{pp}s(t,p), \tag{4a}$$

$$\partial_p s(\,\cdot\,,0) = \partial_p s(\,\cdot\,,\mathrm{K}) = 0, \tag{4b}$$

$$s(0,\,\cdot\,) = s_{\mathrm{ini}}(\,\cdot\,) \in L^2(0,\mathrm{K}), \quad \int_0^{\mathrm{K}} s_{\mathrm{ini}}(p)dp = N, \tag{4c}$$

where $F$ is defined at Eq.(3). This is a realistic population model, structured with respect to the pathogen load, in the absence of pathogen transmission.

### 1.3. Existence of solutions to Eq. (4) and convergence toward stationary state

Let us now prove the existence and uniqueness of solutions to system (4).

**Proposition 1.** *For $s_{\mathrm{ini}} \in L_2(0,\mathrm{K})$, the PDE (4) has a unique solution in $C([0,T],L^2(0,\mathrm{K}))$.*

*Proof.* Consider the unbounded operator $A$ with domain

$$\mathcal{D}(A) = \{w \in H^2(0,\mathrm{K}),\ w'(0) = 0,\ w'(\mathrm{K}) = 0\},$$

such that for all $w \in \mathcal{D}(A)$,

$$A(w) = -(Fw)' + \frac{\sigma^2}{2}w''.$$

Then $-A$ is a regular Sturm-Liouville operator. It follows from [11] that $A$ generates a strongly continuous semigroup on $L^2(0,\mathrm{K})$, which proves the proposition. □

We now prove that system (4) possesses a unique stationary state.

**Proposition 2.** *The PDE (4) has a unique stationary state defined by*

$$s_\infty(p) = \lambda \exp\left(\frac{2}{\sigma^2}\int_0^p F(r)dr\right) \qquad \textit{with} \qquad \lambda = \frac{N}{\displaystyle\int_0^{\mathrm{K}} \exp\left(\frac{2}{\sigma^2}\int_0^p F(r)dr\right)dp}, \tag{5}$$

*where $F$ is defined at Eq.(3).*

*Proof.* The stationary states of model (4) are the solutions of the equation :

$$\partial_p\left(F(p)s_\infty(p) - \frac{\sigma^2}{2}\partial_p s_\infty(p)\right) = 0.$$

Thanks to the definition of $F$ and the boundary conditions, this leads to

$$F(p)s_\infty(p) - \frac{\sigma^2}{2}\partial_p s_\infty(p) = 0.$$

Complemented by the initial condition (4c), this simple ODE has a unique solution given by formula (5). □

Finally, we can show that the solution reaches asymptotically this stationary state.

**Proposition 3.** *The solution of the PDE (4), defined at Prop.1, converges at exponential rate towards the steady state $s_\infty$ defined in Prop. 2.*

*Proof.* We first consider solution $s(t,\cdot)$ of (4) with initial condition in $\mathcal{D}(A)$ as defined in proposition 1, and follow the method proposed by Bolley et al. in [7]. Since the equation is homogeneous, without loss of generality, it can be assumed that

$$V(p) = \frac{2}{\sigma^2}\int_0^p F(r)dr, \qquad\qquad s_\infty(p) = \lambda e^{V(p)}.$$

We consider the $L^2$ weighted norm

$$\|f\|^2_{\mathcal{L}^2(]0,\mathrm{K}[,1/s_\infty)} = \int_0^{\mathrm{K}} f(p)^2 \frac{dp}{s_\infty(p)}$$

and define the function

$$G(t) = \|s(t,\cdot) - s_\infty\|^2_{\mathcal{L}^2(]0,\mathrm{K}[,1/s_\infty)}.$$

As the initial condition is in $\mathcal{D}(A)$, $s(t,\cdot)$ is in $C^1((0,T),\mathcal{D}(A))$ and we can differentiate $G$ with respect to $t$, which leads to

$$G'(t) = 2\int_0^{\mathrm{K}} \left(\frac{s(t,p)}{s_\infty(p)} - 1\right)\partial_t s(t,p)dp = \sigma^2 \int_0^{\mathrm{K}} \left(\frac{s(t,p)}{s_\infty(p)} - 1\right)\partial_p\Big[\partial_p s(t,p) - V'(p)s(t,p)\Big]dp.$$

Then, integrating by parts, using boundary conditions (4b) and the fact that $F(0) = F(K) = 0$, see Eq.(3), we find that

$$\begin{aligned} G'(t) &= -\sigma^2 \int_0^{\mathrm{K}} \partial_p\left(\frac{s(t,p)}{s_\infty(p)} - 1\right)\Big[\partial_p s(t,p) - V'(p)s(t,p)\Big]dp \\ &= -\sigma^2 \int_0^{\mathrm{K}} \left|\partial_p\left(\frac{s(t,p)}{s_\infty(p)} - 1\right)\right|^2 s_\infty(p)dp. \end{aligned}$$

From Poincaré-Wirtinger's inequality for bounded domain with weighted norm (see [8, Lemme 3.3]) applied with $\|.\|_{\mathcal{L}^2(]0,\mathrm{K}[,s_\infty)}$, there exists a constant $\kappa$ depending only on the domain $[0,K]$ and the weight $s_\infty$, such that

$$\kappa \int_0^{\mathrm{K}} \left|\frac{s(t,p)}{s_\infty(p)} - 1\right|^2 s_\infty(p)dp \leqslant \int_0^{\mathrm{K}} \left|\partial_p\left(\frac{s(t,p)}{s_\infty(p)} - 1\right)\right|^2 s_\infty(p)dp.$$

Then, using the expression of $G$ and $G'$, we obtain that

$$G'(t) \leqslant -\kappa\sigma^2 G(t).$$

Finally, by a direct application of the differential form of Gronwall's lemma, one can deduce that for all initial condition in $\mathcal{D}(A)$, the solution $s(t,p)$ of (4) converges when time goes to infinity towards the steady state $s_\infty$, in the sense of $\mathcal{L}^2\left(]0,K[,\frac{1}{s_\infty}\right)$, at rate $e^{-\sigma^2\kappa t}$.
From the density of $\mathcal{D}(A)$ in $L^2(0,K)$ it follows that for all initial condition in $L^2(0,K)$, the (mild) solution $s(t,p)$ of (4) also converges when time goes to infinity towards the steady state $s_\infty$, in the sense of $\mathcal{L}^2\left(]0,K[,\frac{1}{s_\infty}\right)$, at rate $e^{-\sigma^2\kappa t}$. □

### 1.4. **Generalized model adding transmission through an external reservoir**

Our aim in this subsection is to add some exchanges of pathogens between individuals through the environment. The salmonella pathogen can be released in the environment by the infected animals and can contaminate food sources, for example watering troughs. This mechanism creates an external reservoir of pathogens which varies according to the excretion and absorption of salmonella by individuals. Thus, it constitutes a major environmental factor in the spread of pathogens. In order to account for this mechanism, the model (4) is modified into

$$\partial_t s(t,p) = -\partial_p\Big(\big(F(p) + \beta_{\text{in}}(p)r - \beta_{\text{ex}}(p)\big)s(t,p)\Big) + \frac{\sigma^2}{2}\partial^2_{pp}s(t,p), \tag{6a}$$

$$\frac{d\ r(t)}{dt} = -\left(\gamma + \int_0^{\text{K}} s(t,p)\beta_{\text{in}}(p)dp\right) r + \int_0^{\text{K}} s(t,p)\beta_{\text{ex}}(p)dp, \tag{6b}$$

$$\frac{\sigma^2}{2}\partial_p s(t,\text{K}) + \beta_{\text{ex}}(\text{K})s(t,\text{K}) = \frac{\sigma^2}{2}\partial_p s(t,0) - \beta_{\text{in}}(0)r(t)s(t,0) = 0, \tag{6c}$$

$$s(0,\ \cdot\ ) = s_{\text{ini}}(\ \cdot\ ) \in H^1(0,\text{K}), \quad \int_0^{\text{K}} s_{\text{ini}}(p)dp = N, \quad r(0) = r_{\text{ini}} \in \mathbb{R}^+, \tag{6d}$$

where $F$ is defined at Eq.(3).

Here the new variable $r$ denotes the reservoir of pathogens in the environment. In PDE (6a), the term $\beta_{\text{in}}(p)r$ represents the uptake of pathogens from the environment, while $\beta_{\text{ex}}(p)$ stands for the pathogen excretion by individuals. Similarly, in the ODE (6b), the quantity $r(t)s(t,p)\beta_{\text{in}}(p)dp$ indicates the uptake of pathogens from the environment by individuals with pathogen load $p$ and the last term $s(t,p)\beta_{\text{ex}}(p)dp$ describes the increase of the pathogen reservoir induced by individuals with pathogen load $p$. We set $\beta_{\text{in}}(p) = \beta_{\text{in}}\,(\text{K} - p)$ and $\beta_{\text{ex}}(p) = \beta_{\text{ex}}p$, with $\beta_{\text{in}}, \beta_{\text{ex}} > 0$, so that the contamination from the reservoir decreases with the pathogen load whereas the excretion increases with the pathogen load. The positive parameter $\gamma$ is the natural decay rate of the pathogen reservoir. Finally, boundary conditions are modified into Robin boundary conditions in order to ensure the conservation of the total population.

## 2. Numerical results for models (4) without transmission and model (6) with transmission

Our goal in this section is to display and comment some numerical simulations of systems (4) and (6); we will test different initial data and we will compare the solutions of the two models, with or without transmission.

The numerical scheme designed is bases on upwind scheme for the transport term and the time-implicit centered three point scheme for the diffusion part. The simulations have been performed with Python 3 (using Numpy & Scipy) on a 500 cell mesh grid and with the parameters summarized in table (2).

In this theoretical analysis, in the absence of experimental calibration, the parameters $A$, $\alpha$ and $C$ are set to values for which the deterministic model (1) has two well separated non trivial stable equilibria corresponding to the last column in Table 1, in order to obtain a bimodal equilibrium distribution in equation (4), describing the coexistence of high-shedder and low-shedder phenotypes in the population. The parameter $K$ has been chosen arbitrarily, and could be rescaled to reflect another carrying capacity. The logistic threshold $p_\star$ has been tuned to trigger an inflammation into the host gut when the pathogen load gets closed to half the carrying capacity. The diffusion parameter sigma was selected in a range of the same order of magnitude of the transport process, meaning that the stochastic effects during the pathogen infection are not negligible and can impact the pathogen dynamics. The parameters $\beta_{in}$ and $\beta_{ex}$ provides a small inter-host infection rate.

| Parameter | K | $A$ | $\alpha$ | $C$ | $n$ | $p_\star$ | $\sigma$ | $\gamma$ | $\beta_{\text{in}}$ | $\beta_{\text{ex}}$ |
|---|---|---|---|---|---|---|---|---|---|---|
| Value | 5.0 | 0.1 | 0.35 | 1.2 | 50 | 2.15 | 1.75 | 1.0 | 1 | 0.2 |

TABLE 2. Values of the parameters used to perform the simulations presented in section 2.

### 2.1. **Structured population without transmission through a pathogen reservoir**

Figure 1 represents some solutions of the population model (4) structured by pathogen load and without transmission through a reservoir, for the parameters given at Table 2. Three different initial data, shown in dotted blue line in Subfigures 1a, 1b and 1c are considered:

$$s_{\text{ini}}(p) = 0.2, \qquad s_{\text{ini}}(p) = \frac{e^{-p^2/9}}{\displaystyle\int_0^{\text{K}} e^{-p^2/9} dp}, \qquad s_{\text{ini}}(p) = \frac{e^{-(\text{K}-p)^2/9}}{\displaystyle\int_0^{\text{K}} e^{-(\text{K}-p)^2/9} dp}. \tag{7}$$

As expected, for each initial datum, the solution converges towards the theoretical stationary state computed at Eq. (5). This stationary state possesses two maximal values at $p = p_1$ and $p = p_3$, corresponding respectively to the low-shedder and the high-shedder groups and a minimal value at $p = p_2$, the unstable steady state of Eq.(1). However, depending on the initial datum, we can observe some discrepancies in the transient behavior, as noticed on the plots of Subfigures 1d, 1e and 1f representing the evolution with time and pathogen load of the density population $s$.

### 2.2. **Structured population with transmission through a pathogen reservoir**

Figure 2 represents the density population $s$, solution to the structured in pathogen load population system (6), with transmission through a pathogen reservoir. The initial datum used for this simulation is $s_{\text{ini}}(p) = 0.2$ and $r_{\text{ini}} = 0$.

The level sets of the density population $s(t, p)$ with respect to time and pathogen load is plotted in Subfigure 2a. As for the model without the reservoir variable, we can observe that $s(t, p)$ converges towards the stationary state (5). The evolution in time of the reservoir variable $r$ and of the total pathogen load within the population $\displaystyle\int_0^{\text{K}} ps(t, p)dp$ is displayed in Subfigure 2b. Due to the pathogen excretion, the reservoir variable first increases until a maximal value of 0.123 at $t = 1.11$. Then in a second phase, it slightly decreases and tends to stabilize around 0.099. Subfigure 2c shows the comparison between the solution $s(t, p)$ for $t = 5$, in dashed green line, and $t = 10$, in red line, and the stationary state of the model without the reservoir variable, see Eq. (4), in black line. According to this figure, the stationary state for the model with the reservoir variable (red curve) is different from the one without (black line). It can be observed that low and high shedder clusters are shifted and that their sizes are changed. Indeed, the low shedder cluster is centered around the steady state $p_1 \simeq 0.61$ for the model with the reservoir variable, whereas it is centered around the steady state $p_1 \simeq 0.28$ without the reservoir variable. In addition, the low shedder cluster is larger in the sense that it contains more individuals when accounting for the reservoir variable. For the high shedder cluster, the effect is the opposite. Indeed, in the model with the reservoir variable, the cluster is smaller (fewer individuals) and shifted towards a smaller value of pathogen load: $p_3 \simeq 3.43$ instead of $p_3 \simeq 3.71$ without reservoir variable. The increase of the low-shedder average pathogen load may reflect the higher exposure to environmental pathogen, whereas the decrease of high shedder load may come from excretion. Indeed, the degradation of the pathogen in the environment makes the reservoir variable a sink source for intra-host pathogens and pulls the pathogen loads towards lower values.

For this model, stationary states can be computed thanks to some fixed-point technique. However, the proof of the asymptotic convergence towards a stationary state is much more difficult to handle than the proof of Prop.3, due to the coupling with the ODE.

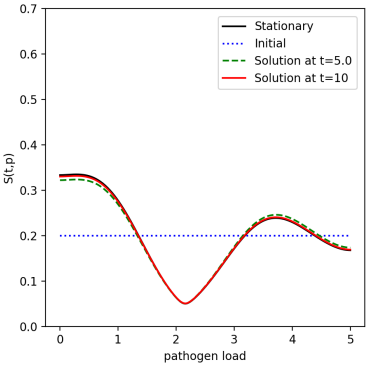


(A) Population density $s$ as a function of pathogen load $p$ at times $t = 5$ and $t = 10$ starting from: $s_{\text{ini}}(p) = 0.2$, compared with the stationary state

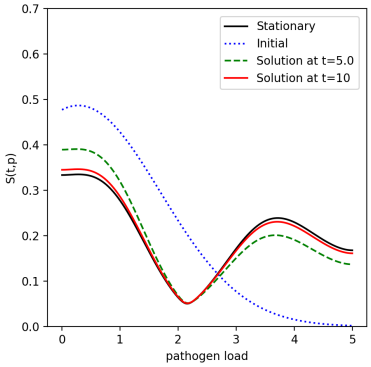


(B) Population density $s$ as a function of pathogen load $p$ at times $t = 5$ and $t = 10$ starting from: $s_{\text{ini}}(p) = \frac{e^{-p^2/9}}{\int_0^{\text{K}} e^{-p^2/9}dp}$, compared with the stationary state

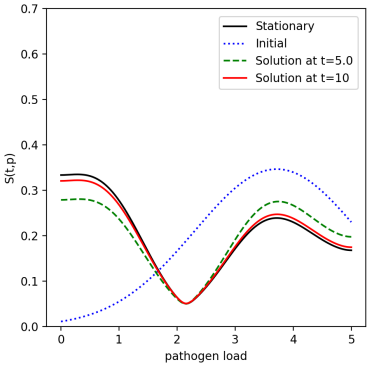


(C) Population density $s$ as a function of pathogen load $p$ at times $t = 5$ and $t = 10$ starting from: $s_{\text{ini}}(p) = \frac{e^{-(\text{K}-p)^2/9}}{\int_0^{\text{K}} e^{-(\text{K}-p)^2/9}dp}$, compared with the stationary state

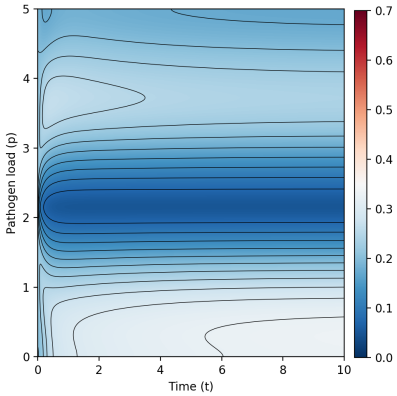


(D) Population density $s$ with respect to time and pathogen load starting from: $s_{\text{ini}}(p) = 0.2$

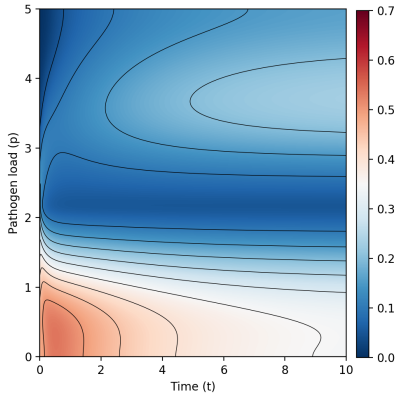


(E) Population density $s$ with respect to time and pathogen load starting from: $s_{\text{ini}}(p) = \frac{e^{-p^2/9}}{\int_0^{\text{K}} e^{-p^2/9}dp}$

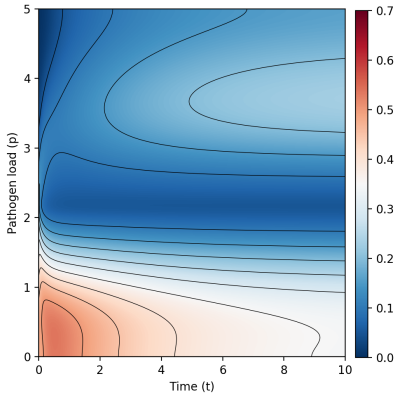


(F) Population density $s$ with respect to time and pathogen load starting from: $s_{\text{ini}}(p) = \frac{e^{-(\text{K}-p)^2/9}}{\int_0^{\text{K}} e^{-(\text{K}-p)^2/9}dp}$

FIGURE 1. Simulations of the structured in pathogen load PDE population model (4) without transmission, for the three different initial data given at Eq. (7). Each column corresponds to one of the initial data, i.e. on the left $s_{\text{ini}}(p) = 0.2$, in the middle $s_{\text{ini}}(p) = \frac{e^{-p^2/9}}{\int_0^{\text{K}} e^{-p^2/9}dp}$, and on the right, $s_{\text{ini}}(p) = \frac{e^{-(\text{K}-p)^2/9}}{\int_0^{\text{K}} e^{-(\text{K}-p)^2/9}dp}$. Top row : initial datum is displayed (dotted blue line), as well as the density population $s$ as a function of pathogen load $p$ at $t = 5$ (dashed green line) and $t = 10$ (red line) and the stationary state (5) (dark line). Bottom row : Level sets of the evolution in time and in pathogen load of the density population $s$ for the same initial data .

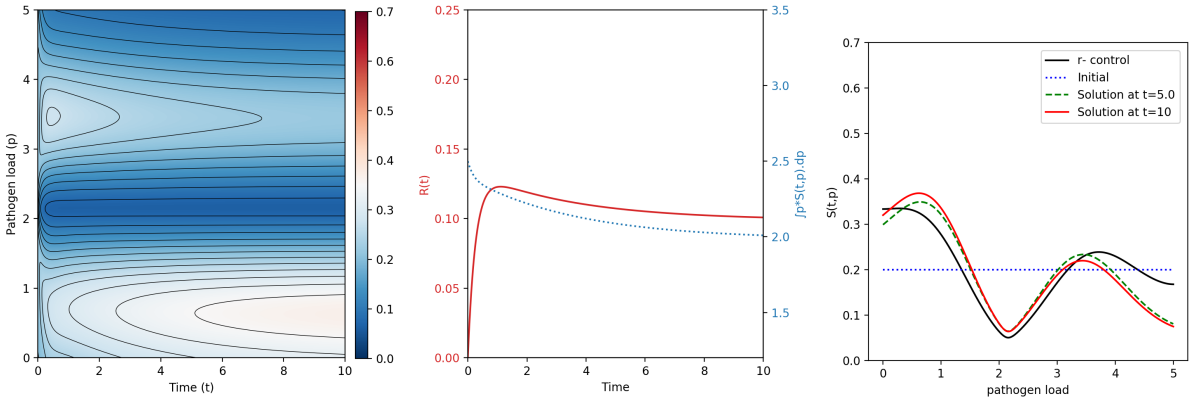


(A) Evolution of $s$ with respect to time and pathogen load

(B) Evolution of reservoir pathogen load $r$ and total pathogen load within the population as functions of time.

(C) Initial datum, population density $s$ as a function of pathogen load $p$ at times $t = 5$ and $t = 10$ compared with the stationary state (5).

FIGURE 2. Numerical simulation of the coupled PDE/ODE system (6), namely the structured in pathogen load population model coupled with the reservoir equation. The initial data are $s_{\text{ini}}(p) = 0.2$ and $r_{\text{ini}} = 0$. Left : level sets of the density population $s$ with respect to time $t$ and pathogen load $p$. Middle : plots of reservoir pathogen load $r$ (red line) and total pathogen load within the population $\int_0^K ps(t,p)dp$ (blue dotted line) as functions of time. Right : Initial datum (blue dotted line), population density $s$ as a function of pathogen load $p$ at times $t = 5$ (green dashed line) and $t = 10$ (red line), compared with the $r^-$ control, i.e. the stationary state without reservoir (5) (black line).

However, we can draw some first conclusions from numerical experiments : for the range of parameters we have tested for $\beta_{\text{in}}$ and $\beta_{\text{ex}}$, the solution always converges towards a steady state. Moreover, whatever the initial datum $s_{\text{ini}}$ chosen among those of Eq.(7) or Dirac masses and whatever $r_{\text{ini}}$, the population density $s$ converges asymptotically towards the same stationary solution.

Consequently, we think that the PDE system (6) possesses only one stable stationary solution and that all solutions converge towards this steady state.

## 3. Study of various control strategies

Control strategies consist in external actions in order to limit the spreading of pathogens within the population. Two types of control will be considered: on the one hand, the cleaning action limits the amount of pathogens in the environment, by removing a certain amount of pathogens represented by the reservoir variable, and, on the other hand, drugs can be used to cure the population. A combination of these two treatments is also considered and a comparison between these three possibilities will be performed.

Let us first describe how to model the two treatment strategies in the PDE system (6).

The cleaning action removes pathogens from the environment. It can be modeled by adding an extra term of the form $-C(t,r)$ in the right hand side of Equation (6b) for the reservoir variable. As a first attempt to describe this mechanism, it is assumed that $C$ is a linear function of $r$, meaning that the cleaning treatment

removes a constant fraction of pathogen reservoir per time unit. Moreover, cleaning might start after a given time and/or might be periodic. Therefore, we assume that $C$ takes the following form :

$$C(t,r) = \rho r(t) \mathbb{1}_{t \in \mathrm{I}_C},$$

where $\rho \in \mathbb{R}^+$ is the cleaning rate and $\mathrm{I}_C$ the time interval(s) during which the cleaning is applied.

On the contrary, the treatment with drugs decreases the pathogen load of the individuals. Therefore this mechanism is modeled by adding an extra term $-T(t,p)s(t,p)$ in the drift term of the population mass balance equation (6a). It is assumed that the treatment removes a constant fraction of the pathogen load of an individual per time unit and that it also depends on time. So, we write the term $T$ accounting for drug treatment as

$$T(t,p) = \theta p \mathbb{1}_{t \in \mathrm{I}_T},$$

where the rate $\theta \in \mathbb{R}^+$ models the treatment efficiency and $\mathrm{I}_T$ the time interval(s) during which the treatment is administrated.

Taking into account cleaning and drug treatment, the system (6) becomes

$$\partial_t s(t,p) = -\partial_p \Big( \big( F(p) + \beta_{\mathrm{in}}(p) r - \beta_{\mathrm{ex}}(p) - T(t,p) \big) s(t,p) \Big) + \frac{\sigma^2}{2} \partial^2_{pp} s(t,p), \tag{8a}$$

$$\frac{d\, r(t)}{dt} = - \left( \gamma + \int_0^{\mathrm{K}} s(t,p) \beta_{\mathrm{in}}(p) dp \right) r + \int_0^{\mathrm{K}} s(t,p) \beta_{\mathrm{ex}}(p) dp - C(t,r), \tag{8b}$$

$$\frac{\sigma^2}{2} \partial_p s(t,\mathrm{K}) + \big( \beta_{\mathrm{ex}}(K) + T(t,K) \big) s(t,\mathrm{K}) = \frac{\sigma^2}{2} \partial_p s(t,0) + \big( T(t,0) - \beta_{\mathrm{in}}(0) r(t) \big) s(t,0) = 0, \tag{8c}$$

$$s(0,\,\cdot\,) = s_{\mathrm{ini}}(\,\cdot\,) \in H^1(0,\mathrm{K}), \quad \int_0^{\mathrm{K}} s_{\mathrm{ini}}(p) dp = N, \quad r(0) = r_{\mathrm{ini}} \in \mathbb{R}^+. \tag{8d}$$

The simulations presented in the following subsections are performed with the parameters of Table 2. We also take $\rho = 5$ for the cleaning rate and $\theta = 0.25$ for the drug treatment rate.

### 3.1. **Cleaning strategy**

Let us begin with the study of the cleaning strategy.

Figures 3 and 4 represent two simulations of system (8) with cleaning only, i.e. $T(t,p) = 0$. For the simulation displayed in Figure 3, the cleaning is activated during the whole simulation, namely $\mathrm{I}_C = \mathbb{R}_+$, whereas in the simulation displayed in Figure 4 the cleaning is only activated on the time interval $\mathrm{I}_C = [10, 20]$.

The results presented in Figure 3 are comparable to the simulation presented in Subsection 2.2. Indeed, in this case, system (8) reduces to system (6) in which the decay rate for the pathogen reservoir $\gamma$ has been shifted to $\tilde{\gamma} = \gamma + \rho$. As in Section 2.2, the system seems to converge towards a stationary state. However, the features previously observed are enhanced. First, we can notice that the population density $s$ affected by cleaning contains more low shedder individuals and less high shedder individuals than the population density without cleaning. In addition, the reservoir variable takes lower values in the case of cleaning; for example, we observe that at time $t = 10$, $r(10) \simeq 0.038$ with cleaning and $r(10) \simeq 0.118$ without cleaning. Similarly, the total pathogen load in the whole population takes lower values, for example, at time $t = 10$, $\int_0^{\mathrm{K}} ps(10,p) dp \simeq 2.0$ without cleaning and $\int_0^{\mathrm{K}} ps(10,p) dp \simeq 1.77$ with cleaning. Finally, the pathogen loads corresponding to low and high shedder individuals are changed ($p_1 \simeq 0.42$ and $p_3 \simeq 3.39$) compared to the model without cleaning ($p_1 \simeq 0.61$ and $p_3 \simeq 3.43$).

Figure 4 displays the results of a simulation where the cleaning is applied only during a range of time $\mathrm{I}_C = [10, 20]$, which allows to study the dynamic response of the system. In Subfigures 4a and 4b , we can notice three different periods of time. The first one corresponds to the time range $t \in [0, 10]$, when the system

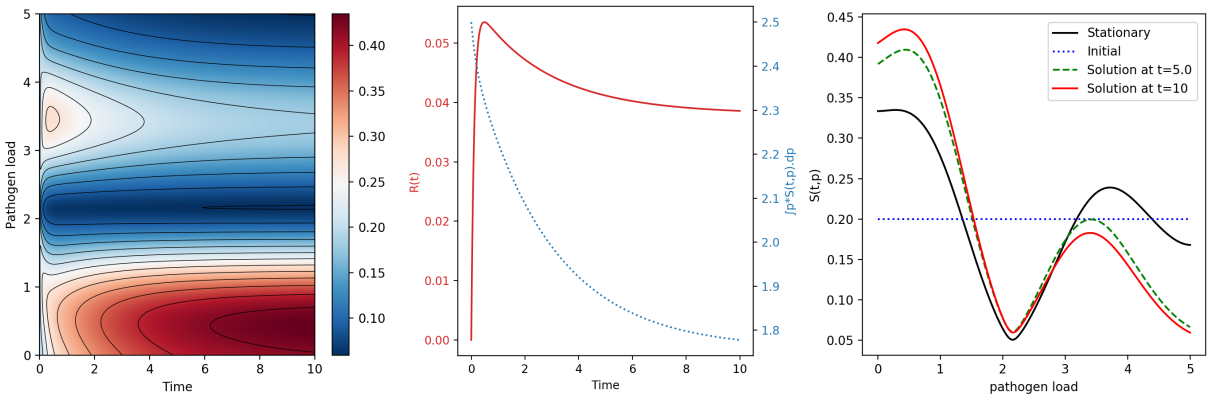


(A) Evolution of $s$ with respect to time and pathogen load with cleaning and without drug treatment.

(B) Evolution of reservoir pathogen load $r$ and total pathogen load within the population as functions of time.

(C) Initial datum, population density $s$ as a function of pathogen load $p$ at times $t = 5$ and $t = 10$ compared with stationary state without reservoir. (5).

FIGURE 3. Simulation of system (8) with cleaning and without drug treatment, namely $T(t,p) = 0$. The cleaning is effective during the whole simulation, i.e. $\mathrm{I}_C = \mathbb{R}_+$. The initial data are $s_{\mathrm{ini}}(p) = 0.2$ and $r_{\mathrm{ini}} = 0$. Left : level sets of the density population $s$ with respect to time $t$ and pathogen load $p$. Middle : plots of reservoir pathogen load $r$ (red line) and total pathogen load within the population $\int_0^{\mathrm{K}} ps(t,p)dp$ (blue dotted line) as functions of time. Right : Initial datum (blue dotted line), population density $s$ as a function of pathogen load $p$ at times $t = 5$ (green dashed line) and $t = 10$ (red line), compared with the stationary state without reservoir (5) (black line).

evolves without cleaning. During this time interval, the system behaves like system (6), see Section 2.2 for the corresponding numerical results. The second period corresponds to $t \in \mathrm{I}_C = [10, 20]$, when the cleaning is applied; according to Figure 4b, the pathogen reservoir rapidly drops off to a range of values similar to those found in the simulation where the cleaning is applied from the beginning, see Figure 3b. On the opposite, the dynamic adaptation of the population is slower. Indeed, as it can be observed in Figure 4b, the total pathogen load $\int_0^{\mathrm{K}} ps(t,p)dp$, plotted in dashed blue line, also decreases but takes a longer time to stabilize. In the last period, which corresponds to $t > 20$, cleaning is removed. Here again, the dynamic adaptation of the pathogen reservoir variable occurs very quickly, whereas the adaptation of the population is slower.

As a conclusion, the cleaning action does not change the global dynamics of the system, but leads to smaller reservoir pathogen levels and lower average pathogen load in the population. Moreover, we can observe that the population dynamic response to cleaning takes more time than the pathogen reservoir dynamic response. Furthermore, when cleaning is stopped, the pathogen distribution rapidly turns back to the distribution observed when no cleaning is applied, showing that cleaning should be applied at a period smaller than this relaxation time scale to be efficient as a control strategy.

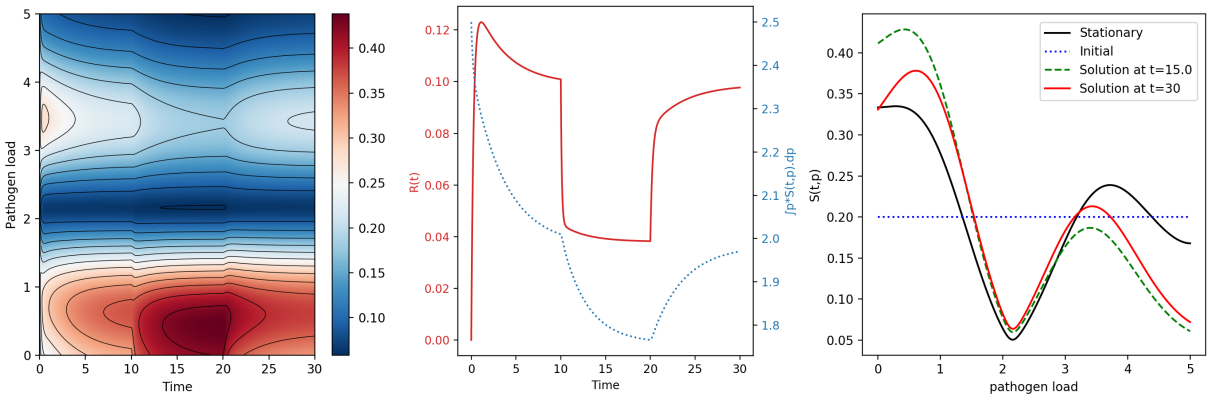


(A) Evolution of $s$ with respect to time and pathogen load with cleaning and without drug treatment.

(B) Evolution of reservoir pathogen load $r$ and total pathogen load within the population as functions of time.

(C) Initial datum, population density $s$ as a function of pathogen load $p$ at times $t = 5$ and $t = 10$ compared with stationary state without reservoir.(5).

FIGURE 4. Simulation of system (8) with cleaning and without drug treatment, namely $T(t,p) = 0$. Cleaning is effective on the time interval $\mathrm{I}_C = [10, 20]$. The initial data are $s_{\mathrm{ini}}(p) = 0.2$ and $r_{\mathrm{ini}} = 0$. Left : level sets of the density population $s$ with respect to time $t$ and pathogen load $p$. Middle : plots of reservoir pathogen load $r$ (red line) and total pathogen load within the population $\int_0^K ps(t,p)dp$ (blue dotted line) as functions of time. Right : Initial datum (blue dotted line), population density $s$ as a function of pathogen load $p$ at times $t = 5$ (green dashed line) and $t = 10$ (red line), compared with the stationary state without reservoir (5) (black line).

## 3.2. **Drug treatment strategy**

In this section, we now consider the effect of a drug treatment and we neglect the cleaning, i.e. $C(t,r) = 0$ in Eq. (8). Two different scenarios of treatment are discussed below.

Figure 5 represents the first scenario in which the treatment is applied for all time, namely $\mathrm{I}_T = \mathbb{R}_+$. According to Figure 5a displaying the population dynamic and Figure 5b representing the pathogen reservoir, the system seems to converge towards a stationary state. The effect of the treatment can be estimated by comparing this simulation with the results obtained in Section 2.2, that is to say the same system without treatment. In Figure 5b, it can be observed that the pathogen reservoir takes lower values in the case with treatment than without, for example $r(10) = 0.053$ with treatment and $r(10) = 0.10$ without. As expected, the total pathogen load in the population is smaller, meaning that the population is less infected by the pathogen when a treatment is administrated. This observation is enforced by comparing the size of the low and high shedder groups in Figure 5c with the ones in Figure 2c. Indeed, with a drug treatment, a large part of the population concentrates around the low shedder pathogen load value $p_1$ and the high shedder group, i.e. individuals with a pathogen load around $p_3$, is smaller. Moreover, the treatment shifts towards lower values the pathogen loads corresponding to low and high shedder individuals, namely $(p_1, p_3) = (0.39, 3.09)$ with the treatment, whereas $(p_1, p_3) = (0.61, 3.43)$ without.

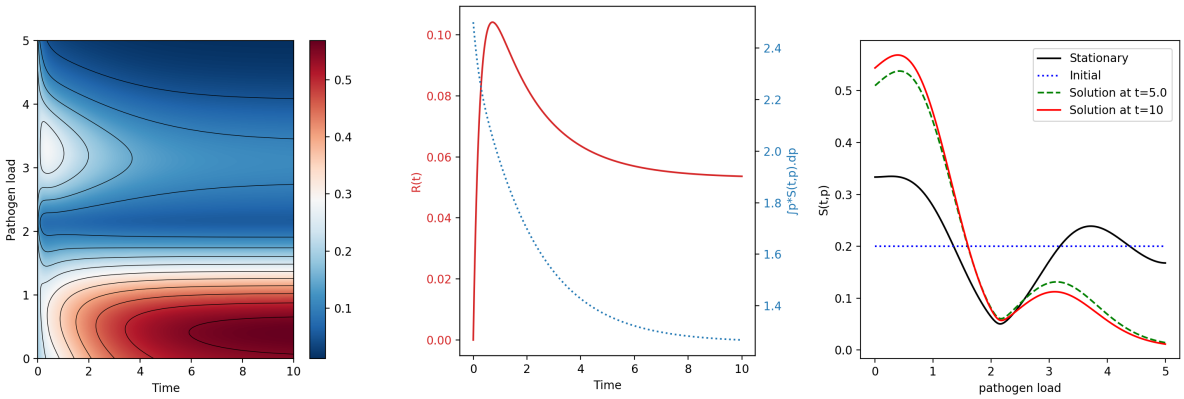


(A) Evolution of $s$ with respect to time and pathogen load with drug treatment and without cleaning.

(B) Evolution of reservoir pathogen load $r$ and total pathogen load within the population as functions of time.

(C) Initial datum, population density $s$ as a function of pathogen load $p$ at times $t = 5$ and $t = 10$ compared with stationary state without reservoir (5).

FIGURE 5. Simulation of system (8) with drug treatment and without cleaning, namely $C(t,p) = 0$. The treatment is applied during the whole simulation, i.e. $\mathrm{I}_T = \mathbb{R}_+$. The initial data are $s_{\mathrm{ini}}(p) = 0.2$ and $r_{\mathrm{ini}} = 0$. Left : level sets of the density population $s$ with respect to time $t$ and pathogen load $p$. Middle : plots of reservoir pathogen load $r$ (red line) and total pathogen load within the population $\int_0^K ps(t,p)dp$ (blue dotted line) as functions of time. Right : Initial datum (blue dotted line), population density $s$ as a function of pathogen load $p$ at times $t = 5$ (green dashed line) and $t = 10$ (red line), compared with the stationary state without reservoir (5) (black line).

In the simulation represented in Figure 6, drug treatment is only applied during the time interval $\mathrm{I}_T = [10, 20]$. As for the cleaning case, this simulation allows to study the dynamic response of the system to the drug treatment and the evolution of the solution in Subfigures 6a and 6b can also be divided into three periods. The first one corresponds to the time range $t \in [0, 10]$ with no cleaning. In this first phase, the system behaves like System (6), see Section 2.2 for the corresponding numerical results. The second time period corresponds to $t \in \mathrm{I}_C = [10, 20]$. During this period, according to Figure 6b, the total pathogen load of the population, plotted in dashed blue line, and the pathogen reservoir decrease exponentially. Remark that, here, both the pathogen reservoir and the total pathogen load within the population decrease with the same exponential rate, unlike what was observed for the cleaning case. In the last period, which corresponds to $t > 20$, the treatment is removed and, as expected, the pathogen reservoir and the total pathogen load increase. Here again, the dynamic adaptation of the pathogen reservoir and the average pathogen load follow an exponential dynamics with a comparable rate. After the end of the therapy, the system recovers its original dynamics, showing again that the administration periodicity is important for a durable effect.

### 3.3. **Combination of cleaning and drug treatment**

We now consider the case when cleaning and drug treatment are combined in order to decrease the pathogen load. A simulation of System (8) with both terms $C(t,r)$ and $T(t,r)$ is displayed at Figure 7. In this simulation,

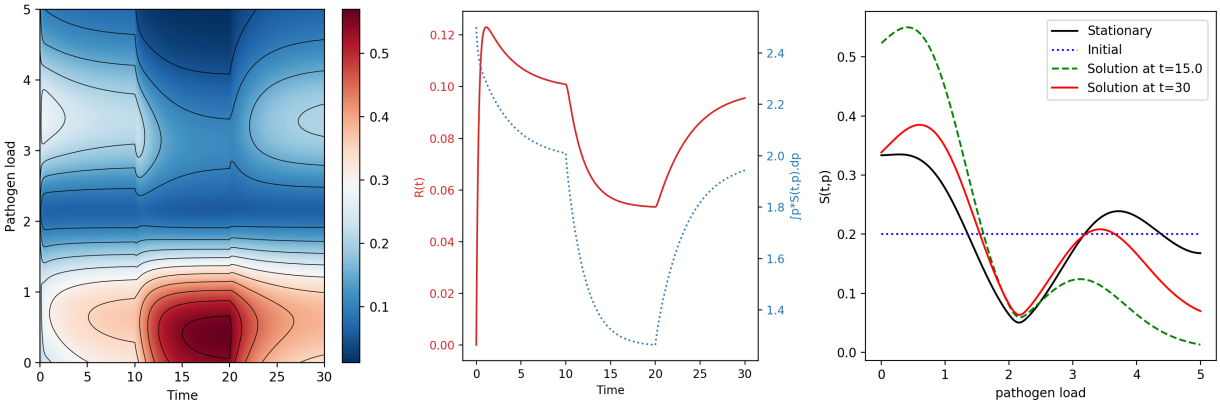


(A) Evolution of $s$ with respect to time and pathogen load with drug treatment and without cleaning.

(B) Evolution of reservoir pathogen load $r$ and total pathogen load within the population as functions of time.

(C) Initial datum, population density $s$ as a function of pathogen load $p$ at times $t = 5$ and $t = 10$ compared with stationary state without reservoir (5).

FIGURE 6. Simulation of system (8) with drug treatment and without cleaning, namely $C(t,p) = 0$. The treatment is applied during the time period $\mathrm{I}_T = [10, 20]$. The initial data are $s_{\mathrm{ini}}(p) = 0.2$ and $r_{\mathrm{ini}} = 0$. Left : level sets of the density population $s$ with respect to time $t$ and pathogen load $p$. Middle : plots of reservoir pathogen load $r$ (red line) and total pathogen load within the population $\int_0^{\mathrm{K}} ps(t,p)dp$ (blue dotted line) as functions of time. Right : Initial datum (blue dotted line), population density $s$ as a function of pathogen load $p$ at times $t = 5$ (green dashed line) and $t = 10$ (red line), compared with the stationary state without reservoir (5) (black line).

cleaning and treatment are activated during the whole time, namely $\mathrm{I}_C = \mathrm{I}_T = \mathbb{R}_+$. The values for the cleaning rate and the treatment rate are the same as in the previous subsections and, as expected, both effects accumulate. Indeed, by comparing Figure 7b with Figures 3b and 5b, it can be observed that the pathogen reservoir and the total pathogen load remain lower than in the cleaning or the drug treatment cases. Here again, it seems that the system converges towards a stationary state, according to Figure 7a.

## 3.4. **Comparison of the various control strategies**

According to the simulations presented in the previous subsections, the cleaning strategy does not allow to decrease efficiently the pathogen load. On the opposite, the drug treatment seems much more efficient and leads to a substantial reduction of the pathogen load in the population. Indeed, cleaning reduces the environmental pathogen load which decreases the positive drift term $\beta_{\mathrm{in}}(p)r$ in Eq. (8a): the impact of cleaning on the pathogen distribution is then driven by the excretion represented by the negative drift $\beta_{\mathrm{ex}}(p)$ which is no longer balanced by the pathogen absorption. The same behavior occurs during drug treatment: the environmental pathogen load is decreased consecutively to the reduction of the high-shedding, and the negative drift $\beta_{\mathrm{ex}}$ also nearly fully applies. However, it is supplemented in that case by the treatment negative drift $T(t,p)$, inducing a stronger impact on the pathogen distribution. Depending on the parameters, the high shedder can be eliminated. However, these conclusions are highly dependent on the chosen parameter values and the modeling of the control strategies is

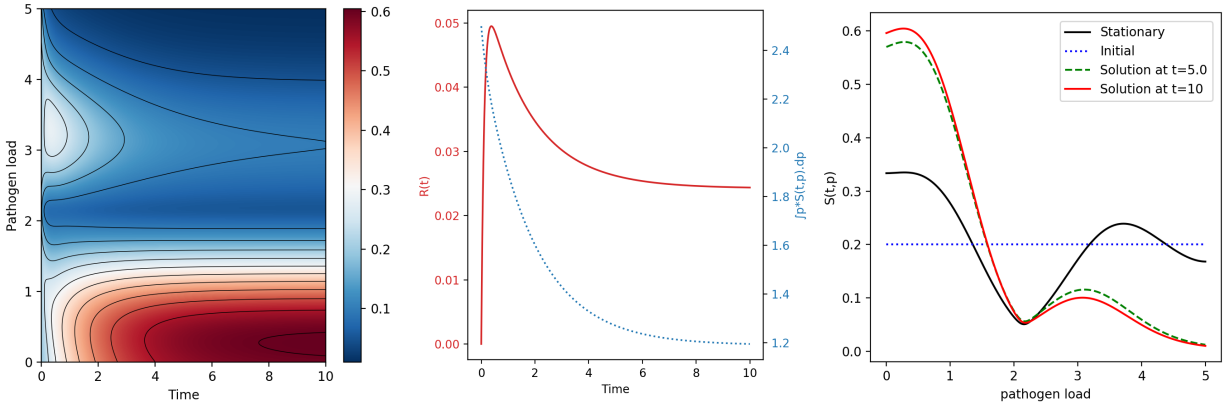


(A) Evolution of $s$ with respect to time and pathogen load with cleaning and drug treatment.

(B) Evolution of reservoir pathogen load $r$ and total pathogen load within the population as functions of time.

(C) Initial datum, population density $s$ as a function of pathogen load $p$ at times $t = 5$ and $t = 10$ compared with stationary state without reservoir (5).

FIGURE 7. Simulation of system (8) with cleaning and drug treatment, namely $T(t,p) \neq 0$ and $C(t,p) \neq 0$. The cleaning and the drug treatment are applied during the whole simulation, i.e. $\mathrm{I}_C = \mathrm{I}_T = \mathbb{R}_+$. The initial data are $s_{\mathrm{ini}}(p) = 0.2$ and $r_{\mathrm{ini}} = 0$. Left : level sets of the density population $s$ with respect to time $t$ and pathogen load $p$. Middle : plots of reservoir pathogen load $r$ (red line) and total pathogen load within the population $\int_0^{\mathrm{K}} ps(t,p)dp$ (blue dotted line) as functions of time. Right : Initial datum (blue dotted line), population density $s$ as a function of pathogen load $p$ at times $t = 5$ (green dashed line) and $t = 10$ (red line), compared with the stationary state without reservoir (5) (black line).

highly simplified. Finally, the combination of cleaning and treatment seems to be, in any case, the most efficient strategy.

## 4. Generalization to a compartment model with transfers

In this section, we generalize the model (6) introduced in Sec. 1.4 by considering compartments. In particular, the compartments can represent different cages (or farms), between which there exist exchanges of animal or/and of the pathogens present in the environment, for example pathogens carried by farming tools.

Let us define $d \in \mathbb{N}^*$ as the number of compartments. From now on,

$$s(t,p) = \big(s_1(t,p), \quad s_2(t,p), \quad \dots, \quad s_d(t,p)\big) \in \mathbb{R}^d$$

will be a vector gathering the populations of the various compartments, structured by pathogen. Similarly, $r(t) = \big(r_1(t), \quad r_2(t), \quad \dots, \quad r_d(t)\big) \in \mathbb{R}^d$ is now the vector gathering the reservoir variables in all the compartments. Moreover, let A, respectively B, be the transfer matrix in $\mathscr{M}_d(\mathbb{R})$ representing the exchanges between compartments for the individuals, respectively for the salmonella pathogen reservoirs. Indeed, for $1 \leqslant i, j \leqslant d$ and $i \neq j$, the coefficient $\mathrm{A}_{i,j} \geqslant 0$ (resp. $\mathrm{B}_{i,j} \geqslant 0$) corresponds to the transfer rate from compartment $j$ to compartment $i$. Because the total population of animals (resp. pathogens in the reservoir) has to be conserved

by the transfers between compartments, the diagonal coefficient $\mathrm{A}_{i,i}$, which corresponds to the total amount leaving the compartment $i$, satisfies $\mathrm{A}_{i,i} = -\sum_{k\neq i} \mathrm{A}_{k,i}$ (resp. $\mathrm{B}_{i,i} = -\sum_{k\neq i} \mathrm{B}_{k,i}$). With these notations, the model writes as

$$\partial_t s(t,p) = -\partial_p\Big(\big(F(p) + \beta_{\mathrm{in}}(p)r - \beta_{\mathrm{ex}}(p)\big)s(t,p)\Big) + \frac{\sigma^2}{2}\partial^2_{pp}s(t,p) + \mathrm{A}s(t,p), \tag{9a}$$

$$\frac{d\ r(t)}{dt} = -\left(\gamma + \int_0^{\mathrm{K}} s(t,p)\beta_{\mathrm{in}}(p)dp\right) r + \int_0^{\mathrm{K}} s(t,p)\beta_{\mathrm{ex}}(p)dp + \mathrm{B}r(t), \tag{9b}$$

$$\frac{\sigma^2}{2}\partial_p s(t,\mathrm{K}) + \beta_{\mathrm{ex}}(K)s(t,\mathrm{K}) = \frac{\sigma^2}{2}\partial_p s(t,0) - \beta_{\mathrm{in}}(0)r(t)s(t,0) = 0, \tag{9c}$$

$$s(0,\ \cdot\ ) = s_{\mathrm{ini}}(\ \cdot\ ) \in H^1(0,\mathrm{K}), \quad \int_0^{\mathrm{K}} s_{\mathrm{ini}}(p)dp = N, \quad r(0) = r_{\mathrm{ini}} \in \mathbb{R}^+. \tag{9d}$$

Let $N(t) = \displaystyle\int_0^{\mathrm{K}} s(t,p)dp$ be the vector of the total population in each compartment. By integrating (9a), one can deduce that $N$ satisfies the ODE $N'(t) = \mathrm{A}N(t)$. Therefore, using Eq.(9d), the population sizes in all compartments are explicitly given by $N(t) = \exp(t\mathrm{A})\,N$, where $N(0) = N = \displaystyle\int_0^{\mathrm{K}} s_{\mathrm{ini}}(p)dp$ is the vector of the initial total populations in the cages. We also remark that the overall total population remains constant since $\big(\sum_i N_i\big)' = \sum_i \big(AN\big)_i = \sum_j (\sum_i A_{i,j})N_j = 0$.

## 4.1. **Numerical simulations for multiple compartments (cages/farms)**

In the following, we will consider the case of 4 compartments and we will perform some numerical simulations. We will first study the case of transfers of individuals without any transfer of reservoir pathogens, then the case of transfers of reservoir pathogens without any transfer of individuals.

### 4.1.1. *Multiple compartments and transfers of individuals*

Here, we investigate the case with no transfers for the reservoir pathogens $r$, that is to say $\mathrm{A} = 0$, and only transfers of individuals between the compartments. This situation may represent a farm where individuals of the same species will be exchanged between different cages or several farms with exchanges of individuals of the same species between them. Therefore, we make the assumption that the populations have the same characteristics in each compartment, i.e. $F$, $\beta_{\mathrm{ex}}$ and $\sigma$ are identical. However, each compartment, cage or farm, may have its own properties and we use therefore different values for the intakes of pathogens from the reservoir $\beta_{\mathrm{in}}$ and for the reservoir decay rate $\gamma$ according to the compartment. In addition, different initial distributions of the population in terms of pathogen load $s_{\mathrm{ini}}(p)$ and various initial conditions of reservoir pathogens $r_{\mathrm{ini}}$ are considered. The corresponding values are gathered in Table 3 and the transfers of individuals between compartments are given by the matrix

$$\mathrm{A} = \begin{pmatrix} -2.25 & 0.75 & 0.75 & 0.75 \\ 0.5 & -1.5 & 0.5 & 0.5. \\ 0.25 & 0.5 & -1.5 & 0.75 \\ 1.5 & 0.25 & 0.25 & -2 \end{pmatrix}. \tag{10}$$

Note that all the rows of A sum to 0 meaning that there is no loss or gain of individuals induced by transfers.

The results of the simulation with these parameters are displayed in Figure 8. As it can be observed in Figures 8a and 8b, the system seems to converge towards a stationary state. In Figure 8b the dashed curves represent the pathogen reservoirs in red and the pathogen population loads $\int_0^{\mathrm{K}} ps(t,p)dp$ in blue as a function of time when the transfers are neglected, whereas the plain curves correspond to the same quantities when the transfers are given by matrix A defined at Eq. (10). Similarly, in Fig. 8c, the black curves correspond to the

| Parameter | Compartment 1 | Compartment 2 | Compartment 3 | Compartment 4 |
|---|---|---|---|---|
| $s_{\text{ini}}(p)$ | 0.2 | $\varphi_0(p)$ | $\varphi_{0.5}(p)$ | $\varphi_1(p)$ |
| $r_{\text{ini}}$ | 0.1 | 0.125 | 0.15 | 0.175 |
| $\beta_{\text{in}}$ | 1.6 | 1.3 | 1.0 | 0.7 |
| $\gamma$ | 0.4 | 0.7 | 1.0 | 1.3 |
| $\sigma$ | 2.45 | 1.4 | 1.75 | 2.1 |

TABLE 3. Values of the intakes of pathogens from the reservoir $\beta_{\text{in}}$, reservoir decay rate $\gamma$, initial distributions of the population in terms of pathogen load $s_{\text{ini}}(p)$ and initial conditions of reservoir pathogens $r_{\text{ini}}$ for the 4 different compartments, used in the simulation represented in Figure 8. The function $\varphi_\alpha(p)$ used to build the initial data is defined by $\varphi_\alpha(p) = \frac{1}{3\sqrt{\pi}} e^{-(\alpha \mathrm{K} - p)^2/9}$.

population distribution $s(t = 10, p)$ as a function of the pathogen load $p$ at time $t = 10$ when the transfers are neglected; the solutions at different times when transfers are taken into account are displayed, namely $s(t = 0, p)$ in blue, $s(t = 5, p)$ in green, and $s(t = 10, p)$ in red. According to these simulations, the transfers of individuals modify the solution. For example, the pathogen reservoir and the total pathogen load for the population in the first compartment are lower than when transfers are accounted. On the opposite, in the second compartment, the pathogen reservoir and the total pathogen load for the population are higher when the transfers are activated. For the third compartment, the dynamics is almost unchanged. Finally, for the fourth compartment, the values at final time $t = 10$ for the pathogen reservoir and the total pathogen load of the population are similar but the transient dynamics is slowed down.

#### 4.1.2. *Multiple compartments and transfers between pathogen reservoirs*

Now, we study the case with no transfers of individuals, that is to say $\mathrm{A} = 0$, and only transfers of reservoir pathogens between the compartments. Transfers of pathogen reservoirs between compartments correspond for example to transfers of pathogens induced by farming activities, for instance by using the same clothes or boots in different buildings on a farm. It can also represent the spreading of the pathogen reservoir by environmental factors, e.g. wind, between farms or cages. In this case, all the parameters can be different from one compartment to another. However, in order to compare the effects of the transfers of the pathogen reservoirs with the transfers of individuals, the simulation presented in Figure 9 has been performed with the same parameters as in previous section, see Table 3. The transfers for the pathogen reservoirs are given by the matrix

$$\mathrm{A} = \begin{pmatrix} -6 & 2 & 1 & 3 \\ 0.25 & -1 & 0.25 & 0.5 \\ 0.5 & 2.5 & -6 & 3 \\ 0.25 & 0.5 & 0.25 & -1 \end{pmatrix}. \tag{11}$$

According to Figures 9a and 9b, the solution seems to converge in time towards a stationary state. The main effect of transfers of the pathogen reservoirs between compartments can be observed in Figure 9b, which compares the pathogen reservoir size and the total pathogen load in the population over time, in plain curves, with the same simulation without transfers, in dashed curves. With transfer matrix A given at Equation (11), we can notice the effects of the pathogen transfers, for example in compartment 4 or for the time range $[0, 2]$ in compartment 1. However, within the range of parameters used in this analysis, the effect of pathogen reservoir transfers is very weak on the population. Indeed, we can remark that the total pathogen load – see Figure 9b – and the stationary states of the pathogen load distribution – see Figure9c – with and without transfers for the reservoir pathogens are almost identical.

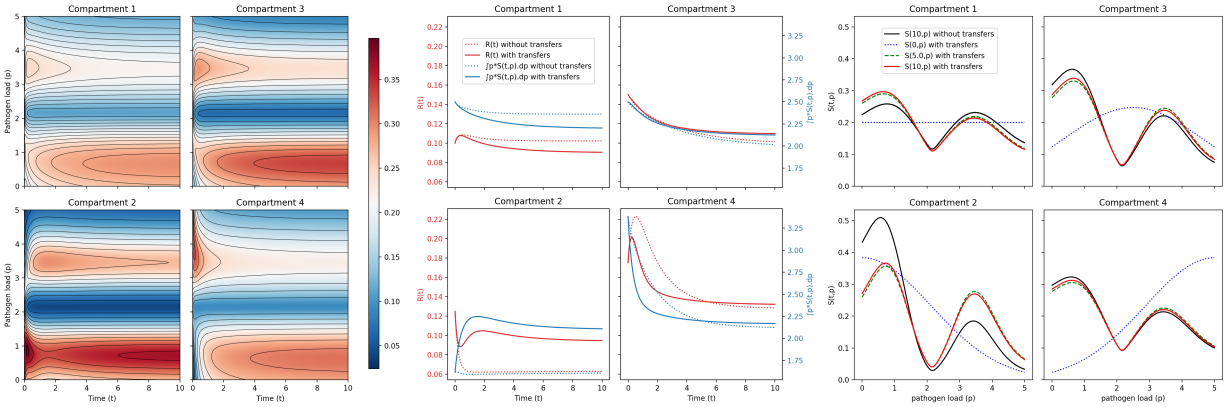


(A) Evolution of $s$ with respect to time and pathogen load in the 4 compartments with $B = 0$.

(B) Evolution of reservoir pathogen load $r$ and total pathogen load within the population in the 4 compartments.

(C) Initial data, population densities $s$ as function of pathogen load $p$ at times $t = 5$ and $t = 10$ compared with stationary state without transfers, in the 4 compartments.

FIGURE 8. Numerical simulation of the coupled PDE/ODE system (9) in 4 compartments, with transfers of individuals given by the matrix (10) and $B = 0$. Values are given at Table 3. Left : level sets of the density population $s$ with respect to time $t$ and pathogen load $p$ in 4 compartments. Middle : plots of reservoir pathogen load $r$ (red line) with or without transfers and total pathogen load within the population $\int_0^K ps(t,p)dp$ (blue line) with or without transfers as functions of time in 4 compartments. Plain lines : case with transfers; dotted lines : case without transfers. Right : Initial data (blue dotted line), population densities $s$ as functions of pathogen load $p$ at times $t = 5$ (green dashed line) and $t = 10$ (red line), compared with the stationary state without transfers (black line) in 4 compartments.

## 4.2. **Towards a continuous model in space**

By considering a large number of compartments and appropriate transfers between them, our model can be seen as a rough approximation of a continuous model in space. For example, the situation where the exchanges between compartments are induced by a diffusion process can be approximated by considering laplacian matrices with periodic boundary conditions for A and B, but with two different diffusion coefficients, namely

$$A = 3\begin{pmatrix} -2 & 1 & 0 & 1 \\ 1 & -2 & 1 & 0 \\ 0 & 1 & -2 & 1 \\ 1 & 0 & 1 & -2 \end{pmatrix} \text{ and } B = \begin{pmatrix} -2 & 1 & 0 & 1 \\ 1 & -2 & 1 & 0 \\ 0 & 1 & -2 & 1 \\ 1 & 0 & 1 & -2 \end{pmatrix}. \tag{12}$$

The parameter values and initial data remain the same as in the two previous subsections and are summarized in Table 3. Here again, we can see at Figure 10 that the solution seems to converge towards a stationary state. Due to the use of diffusion-like transfers, we can observe in Figure 10 that the repartitions of individuals in terms of pathogen loads tend to homogenize. The same kind of homogeneisation can be observed for the reservoir pathogen, its asymptotic values being close in each compartment.

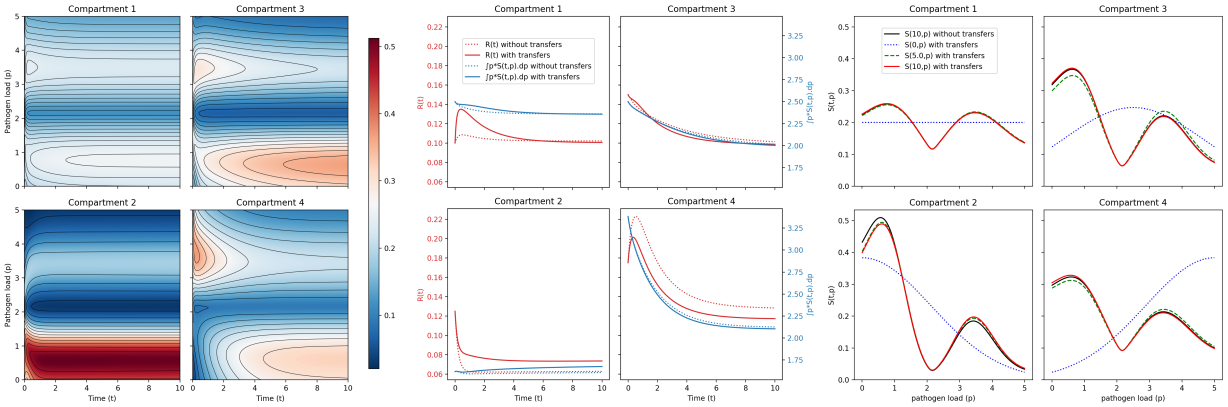


(A) Evolution of $s$ with respect to time and pathogen load in the 4 compartments with A = 0.

(B) Evolution of reservoir pathogen load $r$ and total pathogen load within the population as functions of time in the 4 compartments.

(C) Initial data, population densities $s$ as function of pathogen load $p$ at times $t = 5$ and $t = 10$ and stationary state without transfers, in the 4 compartments.

FIGURE 9. Numerical simulation of the coupled PDE/ODE system (9) in 4 compartments, with transfers for the pathogen reservoir given by the matrix (11) and A = 0. Values are given at Table 3. Left : level sets of the density population $s$ with respect to time $t$ and pathogen load $p$ in 4 compartments. Middle : plots of reservoir pathogen load $r$ (red line) with or without transfers and total pathogen load within the population $\int_0^K ps(t,p)dp$ (blue line) with or without transfers as functions of time in 4 compartments. Plain lines : case with transfers; dotted lines : case without transfers. Right : Initial data (blue dotted line), population densities $s$ as functions of pathogen load $p$ at times $t = 5$ (green dashed line) and $t = 10$ (red line), compared with the stationary state without transfers (black line) in 4 compartments.

## Conclusion and future work

This work is a first step towards a multiscale epidemic model, in which the dymamics of the gut microbiota at the individual level is coupled with a model of pathogen transmission at the population level. The theoretical analysis of the well posedness and convergence of system (6) still needs to be done. A better knowledge of the order of magnitude of some parameters, whose impact on the overall behavior of the models appears to be complex, would be a valuable input. However, in the absence of experimental data for calibration, further works would benefit from a deeper understanding of the effects of each parameter, which could be achieved through the realization of a sensitivity analysis.

## References

[1] M. Byndloss et al. Microbiota-activated PPAR-$\gamma$ signaling inhibits dysbiotic Enterobacteriaceae expansion, Science, 6351(357), 570-575 (2017).
[2] B. Oksendal, Stochastic differential equations. (2003), Springer, Berlin, Heidelberg.
[3] A. Pilipenko, An introduction to stochastic differential equations with reflection (Vol. 1), Universitätsverlag Potsdam, (2014).
[4] Zongo, P., Viet, A. F., Magal, P. and Beaumont, C., A spatio-temporal model to describe the spread of Salmonella within a laying flock, Journal of theoretical biology, 267(4), 595-604 (2010).

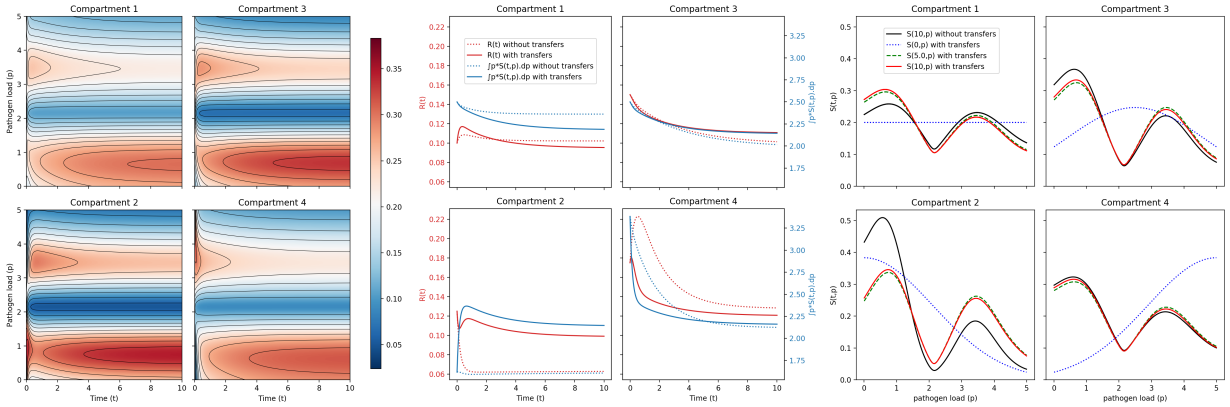


(A) Evolution of $s$ with respect to time and pathogen load in the 4 compartments with B and A given by (12)

(B) Evolution of reservoir pathogen load $r$ and total pathogen load within the population as functions of time in the 4 compartments.

(C) Initial data, population densities $s$ as function of pathogen load $p$ at times $t = 5$ and $t = 10$ compared with stationary state without transfers, in the 4 compartments.

FIGURE 10. Numerical simulation of the coupled PDE/ODE system (9) in 4 compartments, with both transfers for individuals and for the pathogen reservoir given by matrices (12). Values are given at Table 3. Left : level sets of the density population $s$ with respect to time $t$ and pathogen load $p$ in 4 compartments. Middle : plots of reservoir pathogen load $r$ (red line) with or without transfers and total pathogen load within the population $\int_0^K ps(t,p)dp$ (blue line) with or without transfers as functions of time in 4 compartments. Plain lines : case with transfers; dotted lines : case without transfers. Right : Initial data (blue dotted line), population densities $s$ as functions of pathogen load $p$ at times $t = 5$ (green dashed line) and $t = 10$ (red line), compared with the stationary state without transfers (black line) in 4 compartments.

[5] Beaumont, C., Burie, J. B., Ducrot, A. and Zongo, P., Propagation of Salmonella within an industrial hen house, SIAM Journal on Applied Mathematics, 72(4), 1113-1148 (2012).
[6] Zongo, P., Ducrot, A., Burie, J. B. and Beaumont, C. Prevalence of Salmonella in flocks housed in enriched cages, Epidemiology & Infection, 143(6), 1194-1207 (2015).
[7] F. Bolley, I. Gentil, A. Guillin Convergence to equilibrium in Wasserstein distance for Fokker–Planck equations, Journal of Functional Analysis, Volume 263, Issue 8, 15 October 2012, Pages 2430-2457.
[8] S. MISCHLER, Chapitre 1 - Inégalités de Poincaré et de Log-Sobolev, Comportement remarquable d'EDP d'évolution issues de la biologie
[9] Evans, Lawrence C, Partial differential equations, 2nd ed. Providence, RI: American Mathematical Society, 2010. - 749 p.
[10] Curtain, Ruth F, H. Zwart, An Introduction to Infinite-Dimensional Linear Systems Theory, Springer, New York, 1995. - 698 p.
[11] Delattre, C., Dochain, D. and Winkin, J. Sturm-Liouville systems are Riesz-spectral systems, International Journal of Applied Mathematics and Computer Science, 13, 481-484 (2003).
[12] Perthame, B. Transport equations in biology, Springer Science & Business Media (2006).
[13] Buscaglia, G., Ciuperca, I. and Jai, M. Existence and uniqueness for several non-linear elliptic problems arising in lubrication theory, Journal of Differential Equations,218,187-215,(2005).